A Network Pharmacological Study of Chicory in the "Homotherapy for Heteropathy" of Uric Acid Metabolic Diseases

Minghui Niu[1], Zhuang Xu[2], Dingjie Luo[2], Lanfeng Wei[2], Xiaoyu Dong[2], Shuai Chen[2*], Xiaowen Wang[3*]

[1]Pharmacy Intravenous Admixture Services (PIVAs) Shihezi People's Hospital, Shihezi, Xinjiang, China

[2]Xinjiang Key Laboratory of New Energy Materials and Green Chemical Engineering Xinjiang Institute of Engineering, Urumqi, Xinjiang, China;

[3]Xinjiang Zhengsheng Nutrition Research Co., Ltd., Changji, Xinjiang, China.

**Corresponding Author*

Abstract: To decipher the intrinsic regulatory mechanism of chicory in the "homotherapy for heteropathy" of uric acid metabolic diseases using network pharmacology approaches. Methods: TCMSP, HERB, PubChem as well as Swiss Target Prediction, were adopted for the identification of potential compound targets screen the active ingredients and associated targets of chicory. Potential disease targets were acquired using GeneCards and OMIM. Venn diagrams were constructed to identify intersecting targets. The overlapping targets were uploaded to the STRING database for retrieval of protein–protein interaction (PPI) data and subsequent construction of PPI networks. Subsequently, Shared intersective targets were loaded into STRING to obtain comprehensive PPI information, which supported the generation of protein interaction networks. Functional annotation analyses relying on GO and KEGG databases were carried out to characterize the functional features and key pathways associated with screened targets.based on the overlapping targets. Finally, molecular docking and target tissue localization were conducted. Results: Overall 21 bioactive constituents of chicory were yielded, among which quercetin, luteolin, and kaempferol corresponded to relatively high numbers of targets. Sixty-seven intersecting targets between ingredients and diseases were collected. Key targets analyzed by component–target–pathway (C–T–P) and PPI networks were ESR1, TNF, IL6, CASP3, and IL1B. GO enrichment yielded 2353 functional items, and KEGG enrichment yielded 136 pathways. Molecular docking revealed high-binding combinations of key targets as follows: ESR1 with M14, TNF with M13, TNF with M14, IL6 with M13, CASP3 with M3, and IL1B with M1. Tissue localization showed that targets were mainly concentrated in the liver and intestine. Conclusions: As a traditional Chinese medicine, chicory exerts therapeutic effects on uric acid–related metabolic achieve therapeutic intervention on iseases via a synergistic mode featuring multiple phytochemicals and extensive target regulation, multi-pathway, and multi-organ characteristics.

Keywords: Chicory; Network Pharmacology; Homotherapy for Heteropathy; Uric Acid; Metabolic Diseases; Mechanism Study.

1. Introduction

Two representative Asteraceae herbs of genus Cichorium: Cichorium glandulosum Boiss. et Huet. and Cichorium intybus L, two species of the Compositae family, provide the dried aerial parts and roots that are known as chicory — a staple herbal remedy in Uygur and Mongolian medicine. Pharmacologically, this herb is capable of clearing liver heat, enhancing gallbladder performance, invigorating the stomach to facilitate digestion, and promoting urination to eliminate swelling [1-2]. Clinically, it is widely used to treat dysuria, damp-heat hepatitis, systemic edema, and other disorders. In recent years, with in-depth mechanistic research targeting the chemical constituents and pharmacological effects of chicory, it has been found to possess uric acid–lowering, blood glucose–lowering, blood lipid–lowering, anti-gout, and metabolic disorder–improving activities, showing significant therapeutic effects

on various metabolic diseases including obesity, hyperuricemia, and type 2 diabetes mellitus.

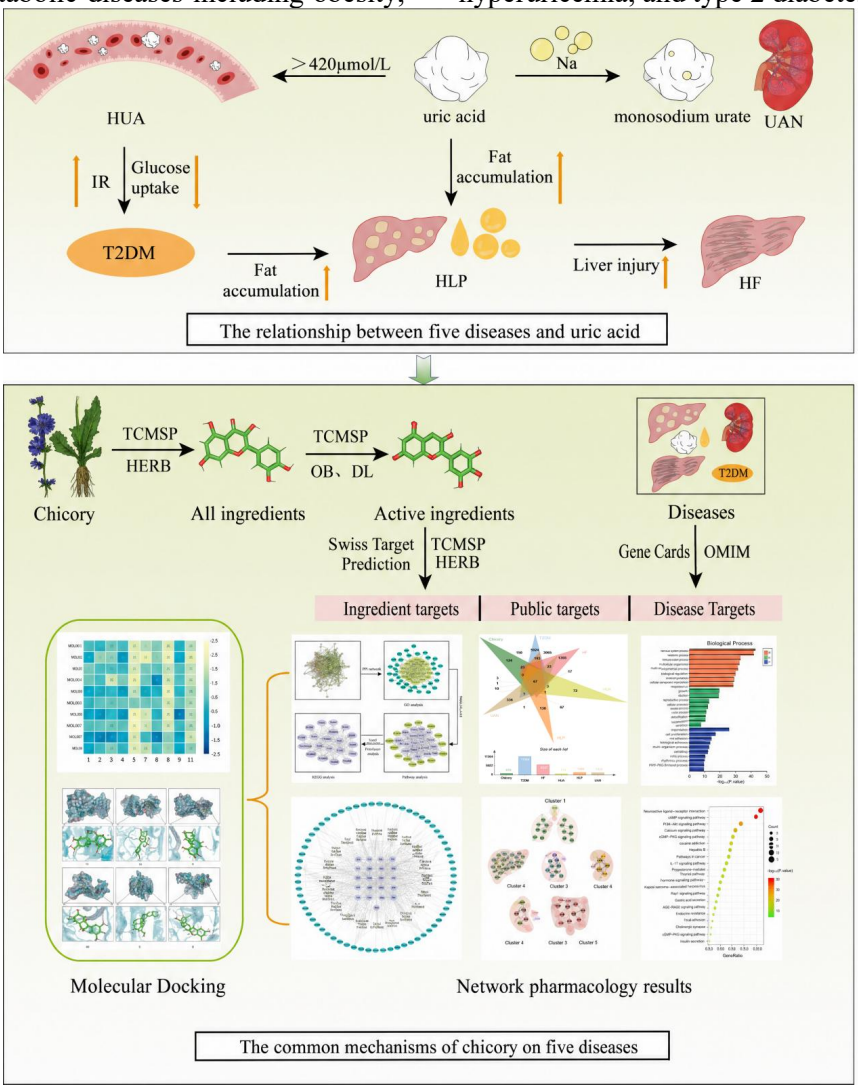

Figure 1. Research Idea

Modern experimental studies indicate that the homeostasis of uric acid metabolism mainly depends on the balance between uric acid production and excretion in the body. Excessive uric acid production and/or reduced excretion lead to abnormally elevated uric acid levels, triggering a series of metabolic diseases such as hyperuricemia, gouty arthritis, and uric acid nephropathy. Numerous clinical studies have demonstrated that many traditional Chinese medicines exert favorable effects on uric acid–related metabolic diseases. Pharmacological experiments have further revealed that various herbal components, including quercetin, lactucopicrin, cichoric acid, chlorogenic acid, and aesculin, regulate uric acid metabolism to varying degrees [3]. At present, no literature has systematically elaborated the common intrinsic regulatory logic governing chicory for the clinical remission of multiple uric acid–related metabolic diseases. To explore its potential common mechanism, we systematically investigated the action characteristics of chicory using network pharmacology, acording to Figure 1.

Network pharmacology is suitable for researching complex diseases with multi-target and multi-effect characteristics, which is highly consistent with the core concepts the core TCM theories covering holistic conception and treatment principles guided by syndrome differentiation [4]. First proposed by Hopkins' team, it can systematically analyze the chemical components and pharmacological properties of traditional Chinese medicines, screen therapeutic targets and explore potential mechanisms of action. Meanwhile, it can clarify the action mechanisms of herbal formulas, single compounds and herb couples.

2. Materials and Methods

2.1 High-Throughput Screening of Pharmacological Components and Functional Target Genes of Chicory

We initially retrieved chemical components of chicory from two public repositorie. Subsequently, the retained chemical constituents underwent further screening on the TCMSP platform. In this study, two classic screening indices were employed to filter bioactive constituents: oral bioavailability (OB) with a threshold of no less than 30% and drug-likeness (DL) with a threshold of no less than 0.18. Such criteria have been extensively recognized for the identification of pharmacologically active molecules with favorable oral absorption characteristics and qualified druggability. Compounds that met the screening requirements were enrolled for subsequent analyses.Three public databases including TCMSP, HERB and SwissTargetPrediction were functioned to collect underlying protein molecular targets of the screened pharmacologically active components. Afterwards, UniProt was employed to normalize all acquired annotated molecular target data and remove redundant data. During the processing, we strictly confined the species to Homo sapiens, retained only the reviewed protein entries from Swiss-Prot, and matched each target with its official gene symbol.

2.2 Collection of Disease Targets

Two well-recognized disease databases, including GeneCards (Version 5.12) as well as the Online Mendelian Inheritance in Man database (OMIM),were used to mine candidate genes associated with five metabolic disorders closely correlated with uric acid metabolism: type 2 diabetes mellitus, liver fibrosis, hyperuricemia, hyperlipidemia and uric acid nephropathy. In the GeneCards dataset, only genes with a relevance score of 10 or above were retained to minimize false positives. All disease-annotated genes were included for subsequent analysis from OMIM. Finally, we merged the target sets of individual diseases and removed duplicates to generate a non-redundant collection of disease-related genes.

2.3 Venn Diagram of Drug–Disease Intersecting Intervention Targets

To facilitate the acquisition of shared targets, we adopted the web-based Venn analysis tool Jvenn to compare target sets of chicory active constituents and disease-associated genes. After uploading the two datasets to the platform, we identified and collected the overlapping molecules. All shared intersective protein targets were identified as potential therapeutic mediators accountable for chicory's pharmacological efficacy and subjected to further systematic analysis.

2.4 Generation of the Protein–Protein Interaction (PPI) Regulatory Network

Aiming to construct the PPI interaction network, we submitted candidate overlapping molecular targets derived from Venn cross-analysis to STRING v11.5. Medium confidence was adopted by fixing the lowest interaction reliability score at 0.4, with all other analytical configurations maintained as factory defaults. Isolated nodes lacking any interacting partners were excluded from the network. Subsequently, Cytoscape 3.7.0 was adopted for network visualization and comprehensive analysis. Three centrality parameters were calculated using the Centiscape 2.2 plugin: degree, betweenness and closeness. Specifically, degree indicates the quantity of direct node connections; betweenness quantifies total number of minimal communication paths traversing a given nteracting molecular entity; closeness is the inverse of the mean distance between any single protein entity within the network and all all remaining interacting protein units within the topological interaction system. According to the median values of the three centrality metrics, we set the screening thresholds as degree > 29, betweenness > 37.49 and closeness > 0.0098. Nodes that met all the above criteria were defined as pivotal molecular components of the protein-protein interaction network.

2.5 Systematic Functional Annotation Enrichment Based on GO and KEGG Databases

The online bioinformatics resource (http://www.bioinformatics.com.cn) was adopted to conduct GO functional enrichment and KEGG signaling pathway enrichment assessments. All 67 intersective target genes were imported into the analytical system, and human was selected as the species background. Functional categories exhibiting $P < 0.05$ were screened as significantly enriched items.

Gene Ontology (GO) enrichment analysis

outcomes were stratified into three canonical functional modules, namely biological process (BP), cellular component (CC), as well as molecular function (MF). Within each functional cluster, the top ten significantly enriched annotation entries were sorted according to the negative base-10 logarithm of P-values, and visualized via horizontal bar charts. As for Kyoto Encyclopedia of Genes and Genomes (KEGG) pathway enrichment profiling, any signaling cascades exhibiting a P-value less than 0.05 were defined as statistically noteworthy enrichment pathways for subsequent interpretation. The top 30 enriched pathways were displayed in bubble charts, in which bubble size corresponded to the quantitative magnitude of annotated genes involved, matched with differentiated color coding depth corresponded to the degree of statistical significance.

2.6 Establishment of Component-Target-Pathway (C-T-P) Regulatory Network

To clarify the regulatory associations among active components, overlapping targets and pivotal signaling pathways, A compound-target-signaling pathway (C-T-P) topological network was established via the Cytoscape software platform 3.7.0. Different shapes were adopted to distinguish diverse nodes: circles corresponded to chicory-derived active ingredients, ellipses indicated intersecting target genes, and inverted triangles represented the twenty leading entries KEGG signaling pathways presenting the highest statistical significance. Pathways associated with cancers and those unrelated to metabolic diseases were excluded from the network.Edges were drawn based on associations derived from the previous analyses (i.e., ingredient-target and target-pathway links). All topological indicators of the molecular association framework were quantified through the NetworkAnalyzer functional tool integrated within Cytoscape software to identify nodes with high Degree centrality, which were considered as key components or targets.

2.7 Computational Simulation of Ligand–Protein Complexation

Molecular docking simulations were implemented to quantitatively assess the binding interactions between pivotal bioactive compounds and hub protein targets predicted from the compound-target-pathway (C-T-P) network. For subsequent docking calculations, we screened the top ten candidate ligands and top ten core protein targets ranked by the highest Degree centrality values within the C-T-P interaction network. Two-dimensional structural data of all screened small-molecule compounds were downloaded in SDF format from the PubChem public chemical database (https://pubchem.ncbi.nlm.nih.gov/), followed by format conversion into standard PDB files via the Open Babel toolkit. As for three-dimensional receptor structures, experimentally resolved protein atomic models were retrieved from the RCSB Protein Data Bank (PDB, https://www.rcsb.org/) or the UniProt knowledgebase. In cases where no crystallographic or cryo-EM-determined protein structures could be acquired, SWISS-MODEL was adopted to construct comparative homology models. Prior to docking simulation, all collected protein structural files underwent standardized preprocessing operations using AutoDockTools 1.5.7, including the elimination of redundant water molecules and supplementation of polar hydrogen atoms.Grid boxes were positioned centrally on the putative binding sites prior to molecular docking, which was implemented via AutoDock Vina. The binding affinity was quantified by the predicted binding energy ($kcal \cdot mol^{-1}$). Compounds with a binding energy value no higher than -5.0 $kcal \cdot mol^{-1}$ were regarded as possessing favorable binding activity. Subsequently, PyMOL (version 2.5) was used for the visualization and structural analysis of optimal docking poses.

2.8 Target Tissue Localization

The GeneCards database was used to investigate the tissue distribution patterns of overlapping target genes. Tissue expression scores were obtained by accessing the TISSUES section of gene expression datasets. Finally, we documented the expression levels of all targets across six vital organs: heart, liver, spleen, lung, kidney and intestine.The average expression score across all tissues for each target was calculated, and if the expression score in a particular organ exceeded the average, that organ was considered to have significant expression for that target. The number of targets showing significant expression in each organ was then counted to generate a tissue localization profile.

3. Results

3.1 Predicted Pharmacologically Functional Components in Chicory

A total of 21 active ingredients were obtained from TCMSP and HERB databases (Table.1). Among them, quercetin corresponded to 46 intersecting targets, luteolin to 25 targets, and kaempferol to 20 targets. The number of intersecting targets acted on by active ingredients was represented by the Degree value.

3.2 Prediction of Drug–Disease Potential Targets

From the Traditional Chinese Medicine Systems Pharmacology Database (TCMSP), 878 predicted binding targets of chicory constituents were compiled, HERB, and Swiss Target Prediction platforms. The numbers of disease targets collected from GeneCards and OMIM databases were 11364 for type 2 diabetes mellitus, 6327 for liver fibrosis, 774 for hyperuricemia, 1488 for hyperlipidemia, and 1332 for uric acid nephropathy. The Jvenn online analytical platform was utilized to generate a Venn graph after inputting constituent-derived targets of chicory and pathogenic gene sets. The overlap between the two datasets contained 67 common molecular targets (Figure 2).

3.3 Assembly of the Protein-Protein Interaction Topological Network

Sixty- seven overlapping gene targets were input imported into the STRING webserver, yielding a protein association framework with 67 nodes, 972 edges, an average node degree of 29, and a confidence score > 0.4. The network was analyzed by utilizing the native Centiscape 2.2 module of Cytoscape, with screening conditions of Degree > 29, Betweenness > 37.49, and Closeness > 0.0098. Twenty key targets were screened, including ALB, TNF, IL6, VEGFA, and IL1B (Figure 3).

Table 1. Active Chemical Constituents of Cichory and Their OB and DL Values

No.	Compound Name	OB	DL	Degree
M1	quercetin	46.43	0.28	46
M2	cyanidin 3-glucoside_qt	58.99	0.24	4
M3	Lactucopicrin	95.31	0.71	9
M4	beta-sitosterol	36.91	0.75	15
M5	ψ-taraxasterol	39.75	0.76	5
M6	kaempferol	41.88	0.24	20
M7	(2R)-3-[3-(5-allyl-2-hydroxyphenyl)-4-hydroxyphenyl]propane-1,2-diol	32.21	0.20	10
M8	2S,2'S-Aurantiamide acetate	39.18	0.54	13
M9	α-Amyrin	39.51	0.76	7
M10	artemisinin	49.88	0.31	6
M11	alpha-Carotene/ beta,epsilon-Carotene	34.51	0.58	14
M12	cichorioside B	32.05	0.80	3
M13	delphinidin	40.63	0.28	18
M14	demethylwedelolactone	72.13	0.43	9
M15	Doradexanthin	38.16	0.54	3
M16	Eseramine	45.89	0.31	11
M17	Gitoxigenin	43.93	0.75	4
M18	isobetanidin	59.73	0.52	1
M19	luteolin	36.16	0.25	25
M20	poriferast-5-en-3beta-ol	36.91	0.75	4
M21	wedelolactone	49.60	0.48	8

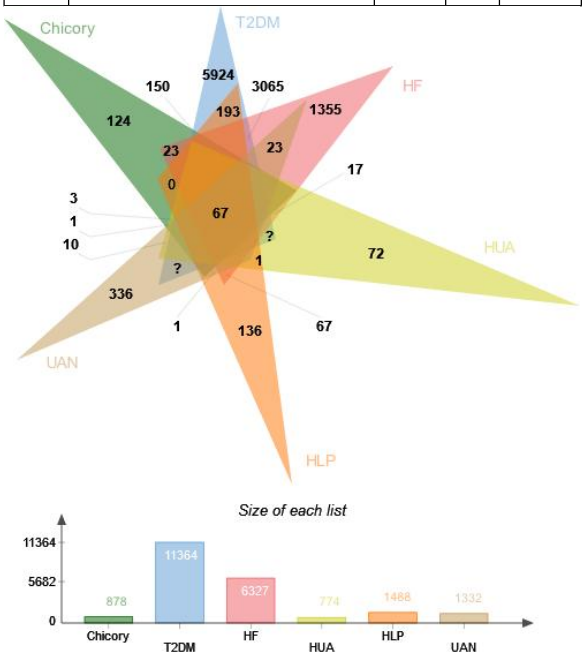

Figure 2. Venn Plot Illustrating Overlapping Molecular Targets between Herbal Medicine and Disease

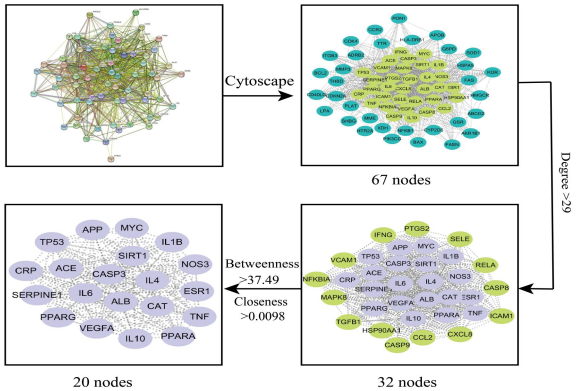

Figure 3. PPI Network Diagram

3.4 Gene Ontology Functional Annotation Coupled with Kyoto Pathway Enrichment Evaluation

Functional enrichment analyses including Gene Ontology (GO) and Kyoto Encyclopedia of Genes and Genomes (KEGG) were conducted on the 67 overlapping target genes via an online bioinformatics analysis platform, with a threshold of $P < 0.05$ for screening significantly enriched entries. A total of 2353 GO functional annotations were identified, among which 149 entries belonged to the molecular function (MF) subclass, such as cytokine receptor binding capacity, cytokine biological activity, as well as signaling receptor agonist activity; 72 terms fell into the cellular component (CC) group, mainly involving membrane lipid rafts, membrane microdomains and regional membrane structures; the remaining 2132 annotations were classified as biological process (BP), covering lipopolysaccharide response, cellular reactions to bacterial metabolites and cellular adaptive responses to biological stimuli. We selected the top 10 significantly enriched entries from each GO subclass based on P-values and visualized them in bar graphs (Figure 4). Collectively, these annotation profiles implied that chicory alleviates hyperuricemia-related metabolic disorders by modulating the above biological functions.

Subsequent KEGG pathway enrichment screening retrieved 136 functional signaling cascades, and the top 30 pathways with prominent enrichment signals were exhibited as bubble diagrams (Figure 5). In this visualization approach, the depth of bubble color correlates negatively with P-values (darker bubbles represent more statistically significant enrichment), while bubble diameter positively reflects the number of enriched target genes participating in corresponding pathways. Within the 30 predominant pathways, 24 were associated with human pathological conditions, encompassing lipid metabolism disturbances coupled with atherosclerosis, the AGE-RAGE signaling axis mediating diabetic complications, fluid shear stress-induced atherosclerotic lesions, Chagas disease and human cytomegalovirus infection pathways. The other six pathways were distributed across three major functional classifications: two signaling axes (TNF and NF-κB signaling) under environmental information processing, two cellular process-related pathways (p53 signal transduction and apoptotic regulatory cascades), as well as two organismal system pathways (IL-17 signaling and Th17 cell lineage differentiation). Taken together, these enrichment observations demonstrate that the therapeutic efficacy of chicory is realized through the coordination of the aforementioned signaling networks.

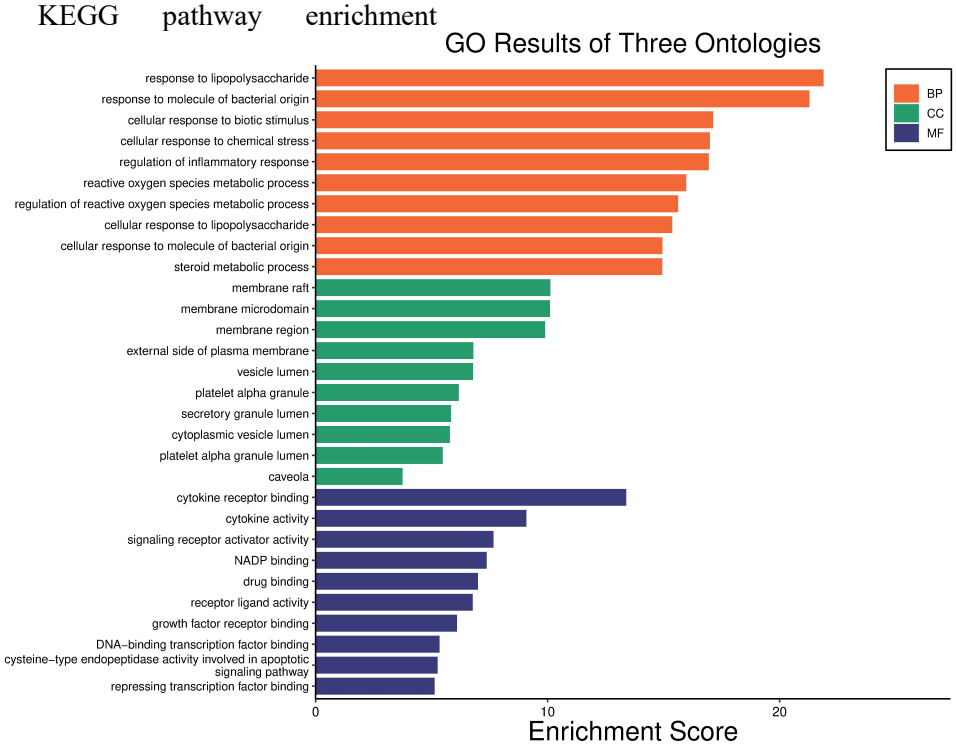

Figure 4. Go Functional Enrichment Analysis Diagram

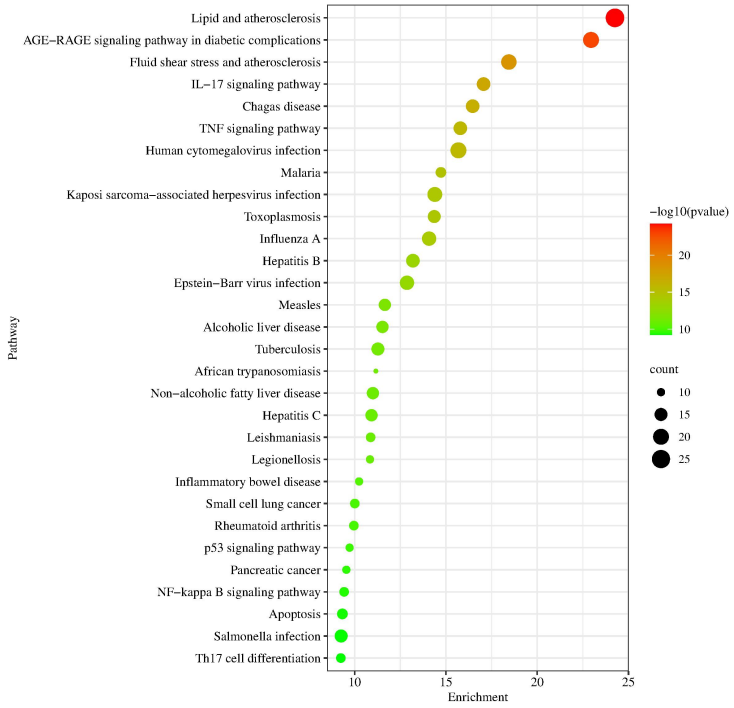

Figure 5. KEGG Pathway Enrichment Bubble Diagram

3.5 Generation of C-T-P Regulatory Association Graph

Drug ingredients, intersecting targets, and information of the top 20 pathways were input iwere imported into Cytoscape 3.7.0 software for topological graph construction. Within this interaction map, circles represent active ingredients, inverted triangles represent pathways, and ellipses represent targets. Network analysis showed that ingredients with top Degree ranks included quercetin, luteolin, kaempferol, delphinidin, and beta- sitosterol; top targets included RELA, MAPK8, ESR1, PTGS2, and NFKB1 (Figure 6).

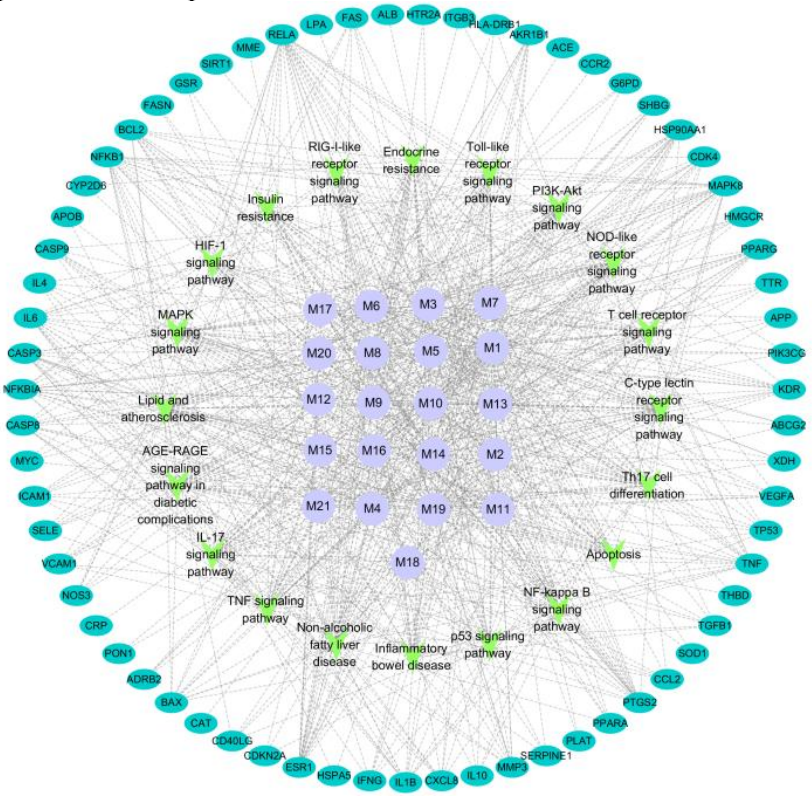

Figure 6. C-T-P Network Diagram

3.6 Active Molecule Docking

Combined with C–T–P and PPI networks, the top 10 targets and compounds were selected for docking, yielding the top 5 combinations with the strongest binding affinity (Figure 7). The combinations were ESR1 and M14, TNF and M13, TNF and M14, IL6 and M13, CASP3 and M3, and IL1B and M1 (Figure 8).

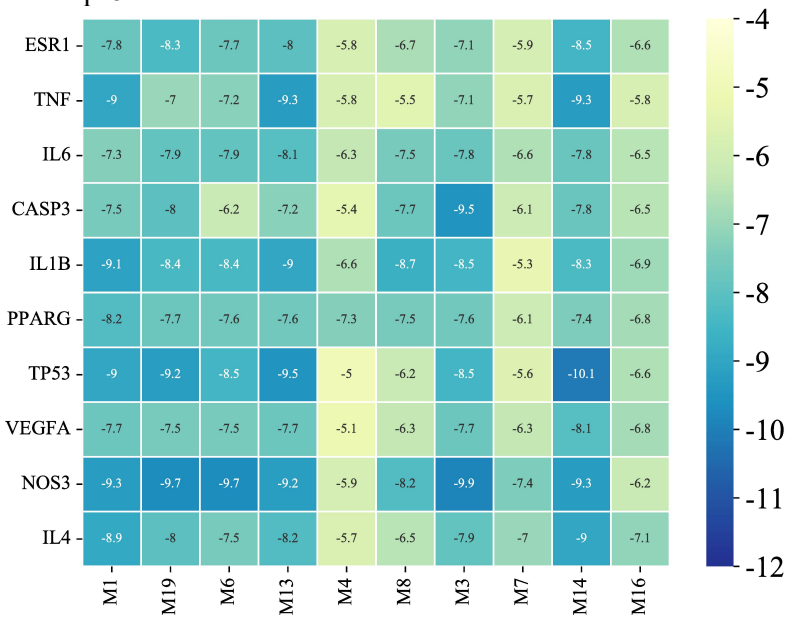

Figure 7. Thermal Map of Molecular Docking Results

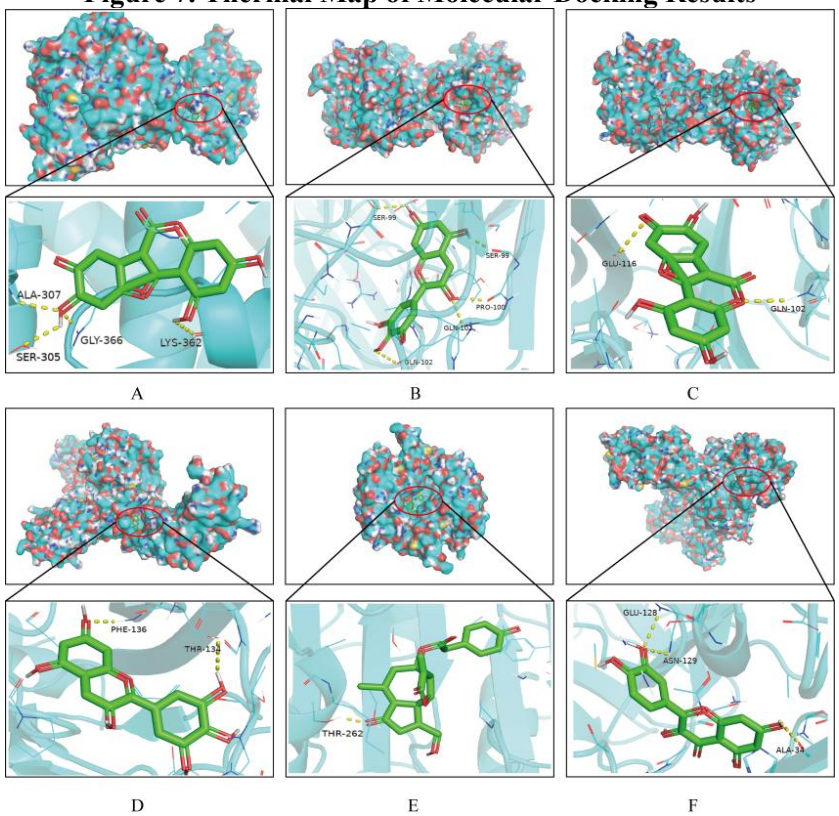

Figure 8. Molecular Docking Diagram with the Best Effect of Key Targets, A: RELA and M14;B: TNF and M13;C: TNF and M14;D: IL6 and M13;E: CASP3 and M3;F: IL1B and M1

3.7 Active Target Tissue Localization

Active target tissue localization was performed using the GeneCards database. Targets were mainly distributed in the liver and intestine, with 52 targets acting on the liver and 46 on the intestine, followed by 36 targets in the kidney (Figure 9).

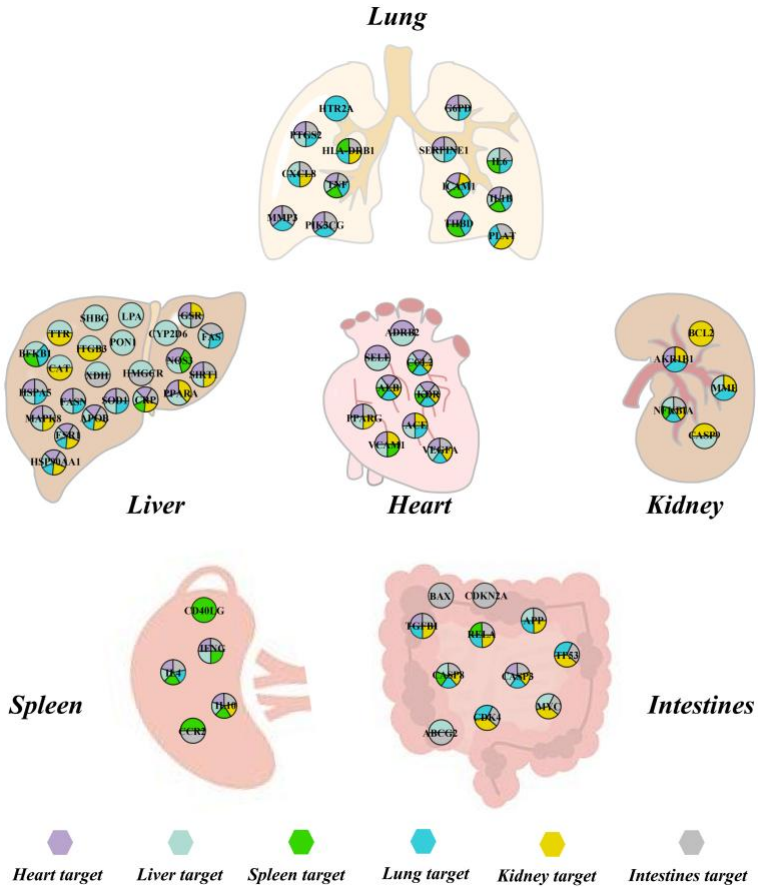

Figure 9 Tissue Localization Diagram of Active Targets

4. Discussion

Network pharmacology approach was adopted to explore the potential therapeutic mechanism of chicory against uric acid-associated metabolic disorders, identifying its main active ingredients as quercetin, luteolin, kaempferol, delphinidin, beta-sitosterol, etc. Modern pharmacological studies have shown that quercetin reduces hepatic XOD activity at a certain dose, enhances the clearance of oxygen free radicals, and reduces uric acid content by inhibiting lipid peroxidation, thereby protecting renal function and preventing renal failure [5]. Luteolin has been found to lower uric acid and ameliorate renal injury induced by hyperuricemia in mice [6]. Kaempferol significantly inhibits xanthine oxidase activity by inserting into its active site and occupying the catalytic center, blocking substrate entry and reducing uric acid production [7]. Moreover, kaempferol exerts therapeutic effects on type 2 diabetes mellitus to a certain extent [8].

Chicory exerts protective effects on uric acid-mediated metabolic diseases through comprehensive interactions with a broad set of target proteins. Based on PPI and C–T–P networks, the five key targets are ESR1, TNF, IL6, CASP3, and IL1B. Literature reports indicate that allelic variation of ESR1 is exhibit prominent correlations with serum estrogen concentrations, insulin signal sensitivity, dyslipidemia and a range of additional metabolic complications [9]. Meanwhile, excessive blood uric acid—due to low solubility—tends to precipitate as monosodium urate and deposit in blood vessels, causing chronic inflammatory injury, damaging vascular intima, increasing the release of TNF and IL6 by vascular-adherent monocytes. Hyperuricemia complicated with glucose and lipid metabolism disorders also elevates serum TNF and IL6 levels [10]. In addition, uric acid significantly inhibits Min6 cell growth, promotes apoptosis, enhances CASP3 activity, and reduces insulin secretion, indicating that CASP3 expression contributes to the treatment of uric acid–related diseases [11]. These analyses suggest that chicory acts on multiple therapeutic targets for uric acid–related diseases, encompassing uric acid-lowering action, suppression of inflammatory responses, and regulatory control over insulin secretion.

Functional enrichment profiling covering Gene Ontology (GO) and Kyoto Encyclopedia of

Genes and Genomes (KEGG) collectively demonstrates that chicory exerts curative impacts on the five targeted illnesses via the synergistic regulation of diverse biological functions and signaling axes. The core therapeutic signaling modules identified herein primarily consist of the AGE-RAGE cascade linked to diabetic complications, IL-17-mediated signal transduction, TNF-associated signaling pathway, alongside the p53 regulatory pathway and other relevant cascades. Accumulated existing research evidence has validated that suppressing the transcriptional and translational level of RAGE protein and intercepting its downstream signal transmission can markedly mitigate endothelial injury and inflammatory overactivation triggered by elevated serum urate levels [12]. The IL-17 signaling pathway is an effective therapeutic pathway for hyperuricemia, as its ligand binding increases inflammatory factor release [13]. Numerous studies have confirmed that the five diseases involved in this study are all associated with inflammatory responses. The TNF signaling pathway regulates inflammatory factors for instance, the pro-inflammatory factors IL-1 and IL-6 by means of mediating circulating eosinophils and peripheral lymphocytes, thereby affecting the intensity of inflammatory responses [14]. This network pharmacological study demonstrates that chicory exerts a common therapeutic effect on the five uric acid–related diseases through multiple pathways. Some pathways have been reported in partial diseases, while most lack experimental verification and require further pharmacological validation.

According to in silico docking assays, prominent binding affinity exists between candidate bioactive components and central target proteins, whose binding energies were all below < -5.0 kcal·mol-1. Compounds with high binding affinity mainly include demethylwedelolactone, delphinidin, lactucopicrin, and quercetin. Literature indicates that lactucopicrin lowers uric acid by inhibiting the purine transport activity of CNT2 and reducing intestinal purine absorption [15]. Quercetin at a certain dose improves renal inflammation by inhibiting NLRP3 inflammasome activation and ameliorates hyperuricemia, dyslipidemia, and renal insufficiency by inhibiting the production of pivotal pro-inflammatory factors, namely IL-1β, IL-6, and IL-18 [16].

Active target tissue localization shows that intersecting targets are mainly concentrated in the liver and intestine. Pharmacological studies have demonstrated that active components of chicory significantly reduce elevated uric acid, blood glucose, and serum triglycerides induced by hyperglycemia. The main mechanism may involve inhibiting hepatic fatty acid synthase activity, reducing serum free fatty acid levels, and upregulating myocardial lipoprotein lipase and hepatic lipase activities to coordinately regulate the reciprocal disorders of glucose, lipid, and uric acid metabolism [17]. In addition, both the kidney and intestine participate in uric acid excretion, and uric acid can be eliminated via feces. Components in chicory inhibit intestinal CNT2 activity and reduce intestinal purine absorption [15]. In summary, ogans with abundant distribution of core target proteins overlap with the major sites exerting medicinal effects. This phenomenon provides additional evidence for the holistic regulatory characteristic of TCM: multiple bioactive constituents simultaneously modulate diverse targets to act on various bodily organs.

5. Conclusions

Based on systematic network pharmacological exploration, chicory can alleviate five kinds of metabolic illnesses triggered by abnormal urate metabolism, which relies on its poly-ingredient, pleiotropic-target and multi-signaling pathway pharmacological characteristics. Twenty-one bioactive constituents were identified, with quercetin, luteolin, and kaempferol being major contributors. In the present study, 67 shared targets and five hub targets (ESR1, TNF, IL6, CASP3, IL1B) were screened out. According to pathway enrichment profiling, the AGE-RAGE, TNF, IL-17 and p53 pathways were markedly overrepresented. Each of these signaling modules exerts critical regulatory roles in inflammatory reactions and metabolic activities. Molecular docking assays verified strong binding activities of candidate compounds. Tissue localization analysis identified the liver and intestine as the principal target organs. In summary, chicory achieves the efficacy of "homotherapy for heteropathy" in the treatment of uric acid metabolic diseases via comprehensive network modulation. The findings lay a theoretical foundation for its clinical application, and follow-up experimental verification is necessary.

Acknowledgements

Sponsored by Regional Collaborative Innovation Special Project Science and Technology Assistance to Xinjiang Project, Research on Key Technologies and Product Development for Processing Functional Foods Derived from Chicory (2025X08).

References

[1] Yang Z , Lyu B , Ma B , et al. Screening of the effective sites of Cichorium glandulosum against hyperuricemia combined with hyperliSSpidemia and its network pharmacology analysis.Computational Biology & Chemistry, 2024, 110(000).

[2] Street R A, Sidana J, Prinsloo G. Cichorium intybus: Traditional uses, phytochemistry, pharmacology, and toxicology. Evid-Based Complementary Altern Med, 2013, 2013(6):579319.

[3] Cheng-Yuan W, Jian-Gang D .Research progress on the prevention and treatment of hyperuricemia by medicinal and edible plants and its bioactive components. Frontiers in Nutrition, 2023, 10(000):14.

[4] Zhang GB, Li QY, Chen QL, et al. Network pharmacology: a new approach for chinese herbal medicine research. Evid Based Complement Alternat Med, 2013, 2013: 621423.

[5] Yao F, Zhang R, Fu R, et al. Preventive and therapeutic effects of quercetin on hyperuricemia and renal injury in rats. Wei sheng yan jiu Journal of hygiene research, 2011, 40(2):175.

[6] Luteolin ameliorates hyperuricemic nephropathy by activating urate excretion and Nrf2/HO-1/NQO1 antioxidant pathways in mice.Food science & nutrition, 12(10):8053-8066.

[7] Wang Y, Zhang G, Pan J, et al. Novel insights into the inhibitory mechanism of kaempferol on xanthine oxidase. J Agric Food Chem, 2015, 63(2): 526-34.

[8] Alshehri A S .Kaempferol attenuates diabetic nephropathy in streptozotocin-induced diabetic rats by a hypoglycaemic effect and concomitant activation of the Nrf-2/Ho-1/antioxidants axis. Archives of Physiology and Biochemistry, 2021(740671):1-14.

[9] Wang W, Liou TH, Lee WJ, et al. ESR1 gene and insulin resistance remission are associated with serum uric acid decline for severely obese patients undergoing bariatric surgery. Surg Obes Relat Dis. 2014, 10(1):14-22

[10] Zhou Y M, Zhao M, Pu Z, et al. Relationship between oxidative stress and inflammation in hyperuricemia: Analysis based on asymptomatic young patients with primary hyperuricemia. Medicine, 2018, 97(49):8.

[11] Jiang Z, Wang G, Meng L, et al. Protective Effects of Astragaloside IV on Uric Acid-Induced Pancreatic β-Cell Injury through PI3K/AKT Pathway Activation. Evidence-Based Complementary and Alternative Medicine, 2022, 2022:2429162.

[12] Wei C , Xi-Mei D , Ying L ,et al. Uric Acid Induces Endothelial Dysfunction by Activating the HMGB1/RAGE Signaling Pathway. BioMed Research International, 2017, 2017:4391920.

[13] Liu P, Xu H, Shi Y, et al. Potential molecular mechanisms of plantain in the treatment of gout and hyperuricemia based on network pharmacology. Evidence-Based Complementary and Alternative Medicine, 2020, 2020: 3023127.

[14] Yuan X, Li N, Zhang M, et al. Taxifolin attenuates IMQ-induced murine psoriasis-like dermatitis by regulating T helper cell

[15] Yue Z, Bing Z, Zhi-Jian L, et al. Virtual screening for components in Chicory combined with CNT2 target based on molecular docking. China Journal of Chinese Materia Medica, 2016, 41(21):3962.

[16] Nutmakul T. A review on benefits of quercetin in hyperuricemia and gouty arthritis. Saudi Pharm J, 2022, 3(7): 918-926.

[17] Hui L I, Liu X Q, Zhang B, et al. Effects of active component in Cichorii on lipid metabolism of rat with hypertriglyceridemia complicated by hyperuricemia and hyperglycemia. Journal of Integrative Medicine (JIM), 2008, 6(2):157

